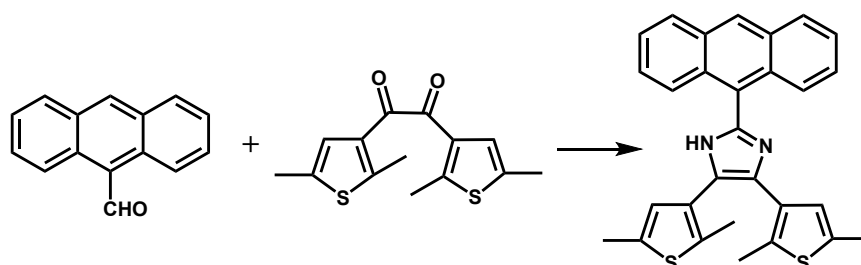


## Electronic Supporting Information

### Materials and methods

1,2-Bis[2,5-dimethyl(3-thienyl)]ethane-1,2-dione was synthesized according to the literature method.<sup>S1</sup> All other reagents were commercially available and used without further purification. Elemental analyses were performed on a Perkin Elmer 240C elemental analyzer. The IR spectra were obtained as KBr disks on a VECTOR 22 spectrometer. The ATR IR spectra of 1 before and after grinding were measured on a NICOLET IS10 spectrometer. The <sup>1</sup>H NMR spectra were recorded at room temperature with a 500 MHz BRUKER AM-500 spectrometer. The powder XRD patterns were recorded on a BRUKER D8 ADVANCE X-ray diffractometer. Diffuse reflectance UV-vis spectra were measured on SHIMADZU UV-3600 spectrophotometer using barium sulfate as the reference. Solid-state luminescence spectra were measured at room temperature on a Perkin Elmer LS55 fluorescence spectrometer. The luminescence spectra of solutions were measured at room temperature on a Hitachi F-4600 fluorescence spectrometer. The luminescent lifetimes were measured at room temperature on an Edinburgh FL-FS920 fluorescence spectrometer.

### Synthesis of 2-(anthraceneyl)-4,5-bis(2,5-dimethyl(3-thienyl))-1*H*-imidazole (anbdtiH)



A mixture of 9-anthracenecarboxaldehyde (1.7 mmol, 0.3506 g), ammonium acetate (17 mmol, 1.3103 g), 1,2-bis[2,5-dimethyl(3-thienyl)]ethane-1,2-dione (1.7

mmol, 0.4732 g), and glacial acetic acid (15 mL) was refluxed for 24 hours. The solvent was removed under vacuum, and then the residue was mixed with H<sub>2</sub>O (10 mL). The resultant mixture was extracted with CH<sub>2</sub>Cl<sub>2</sub> (25 mL × 3). The combined CH<sub>2</sub>Cl<sub>2</sub> solution was dried with MgSO<sub>4</sub>, filtrated, and evaporated under vacuum. The residue was purified through flash column chromatography using ethyl acetate–petroleum ether solution (v/v = 10/90), obtaining yellow solid with a yield of 630 mg (80% based on 9-anthracenecarboxaldehyde). <sup>1</sup>H NMR (500 MHz, CDCl<sub>3</sub>, Figure S1), δ (ppm): 2.21 and 2.42 (12H from 4CH<sub>3</sub>), 2.04 (2H from two thiophene rings), 7.43–8.52 (9H from anthracene group).

### **Preparation of anbdtiH·CHCl<sub>3</sub> (1)**

The CHCl<sub>3</sub> solution of anbdtiH was allowed to slowly evaporate, forming colorless needlelike crystals as a monophasic material based on the powder XRD pattern (Figure S3). Anal. found (calcd) for C<sub>30</sub>H<sub>25</sub>Cl<sub>3</sub>N<sub>2</sub>S<sub>2</sub>: C, 61.57 (61.70); H, 4.52 (4.31), N, 4.71 (4.80). IR (KBr, cm<sup>-1</sup>): 3406(br, m), 3135(br, s), 2919(w), 2856(w), 1683(w), 1615(w), 1399(s), 1143(w), 1048(s), 835(w), 784(w), 727(w), 676(w), 609(w), 562(w).

### **Preparation of anbdtiH·2CH<sub>3</sub>OH (2)**

The sample of anbdtiH was dissolved in CH<sub>3</sub>OH. The filtrate was allowed to slowly evaporate, obtaining colorless lamellar crystals as a monophasic material based on the powder XRD pattern (Figure S4). Anal. found (calcd) for C<sub>31</sub>H<sub>32</sub>N<sub>2</sub>O<sub>2</sub>S<sub>2</sub>: C, 70.30 (70.42); H, 5.98 (6.10), N, 5.42 (5.30). IR (KBr, cm<sup>-1</sup>): 3441(br, s), 3196(br, s), 2914(w), 2806(w), 1626(m), 1434(m), 1401(s), 1308(w), 1207(w), 1137(w), 1032(m), 1010(w), 956(w), 923(w), 884(w), 830(w), 790(w), 735(m), 676(w), 629(w), 606(w), 515(w).

### **Preparation of anbdtiH<sub>2</sub>·CF<sub>3</sub>COO·CH<sub>3</sub>OH·H<sub>2</sub>O (3)**

A mixture of anbdtiH (100 mg) and CF<sub>3</sub>COOH (0.5 mL) in CH<sub>3</sub>OH (10 mL) was stirred for 2 hours. The resultant clear solution was allowed to slowly evaporate,

obtaining colorless blocky crystals as a monophasic material based on the powder XRD pattern (Figure S5). Anal. found (calcd) for  $C_{32}H_{31}F_3N_2O_4S_2$ : C, 61.07 (61.13); H, 4.83 (4.97), N, 4.52 (4.46). IR (KBr,  $cm^{-1}$ ): 3409(s), 3060(m), 2916(m), 2607(m), 1952(w), 1666(s), 1587(s), 1480(w), 1418(m), 1379(m), 1248(w), 1192(s), 1137(s), 977(m), 903(w), 833(w), 790(w), 732(m), 580(w), 502(w), 451(w).

### Preparation of **3-dimer**

Compound **3** (150 mg) was placed in a NMR tube, and was irradiated for 16 hours with sunlight at environment temperature around 30 °C (using sunlight with the time range of 12:00 - 17:00 in sunny days in summer). After finishing irradiation, the solid sample was washed with DMSO (1 mL  $\times$  6), and dried under reduced pressure, obtaining white powder **3-dimer** with a yield of 69 mg (54% based on compound **3**). The DMF-CH<sub>3</sub>OH (v/v = 1/1) solution of **3-dimer** was allowed to slowly evaporate at room temperature, obtaining colorless blocky crystals of **3-dimer·2DMF**. Anal. found (calcd) for  $C_{64}H_{62}O_2N_6S_4$ : C, 71.57 (71.48); H, 5.73 (5.81), N, 8.02 (7.81). IR (KBr,  $cm^{-1}$ ): 3417(s), 3135(br, s), 1680(w), 1620(w), 1399(s), 1147(w), 826(w), 777(w), 693(w), 581(w), 491(w); <sup>1</sup>H NMR of **3-dimer·2DMF** (500 MHz, CDCl<sub>3</sub>, Figure S2),  $\delta$  (ppm): 2.11, 2.36, 2.47, and 2.58 (24H from 8CH<sub>3</sub> attached to four thiophene rings), 2.85 and 2.94 (12H from 4CH<sub>3</sub> in two DMF molecules), 6.37–7.20 (22H from anthracene-dimer moiety and four thiophene rings), 7.93 (2H from two CHO group in two DMF molecules).

### X-ray crystal structure studies

Single crystals of dimensions 0.30  $\times$  0.15  $\times$  0.10 mm<sup>3</sup> for **1**, 0.30  $\times$  0.25  $\times$  0.08 mm<sup>3</sup> for **2**, 0.24  $\times$  0.20  $\times$  0.15 mm<sup>3</sup> for **3**, and 0.15  $\times$  0.12  $\times$  0.10 mm<sup>3</sup> for **3-dimer·2DMF**, were used for structural determinations on a Bruker SMART APEX CCD diffractometer using graphite-monochromatized Mo K $\alpha$  radiation ( $\lambda$  = 0.71073 Å) at room temperature (296 K). A hemisphere of data were collected in the  $\theta$  range of 1.69-27.53° for **1**, 0.95-26.00° for **2**, 1.01-25.00° for **3**, and 1.68-25.00° for **3-dimer·2DMF** using a narrow-frame method with scan widths of 0.30° in  $\omega$  and an

exposure time of 10 s / frame. Numbers of observed and unique [ $I > 2\sigma(I)$ ] reflections are 27790 and 5647 ( $R_{\text{int}} = 0.1014$ ) for **1**, 16465 and 5678 ( $R_{\text{int}} = 0.0693$ ) for **2**, 16697 and 5497 ( $R_{\text{int}} = 0.0234$ ) for **3**, and 22332 and 5055 ( $R_{\text{int}} = 0.1400$ ) for **3-dimer·2DMF**, respectively. The data were integrated using the Siemens *SAINT* program,<sup>S2</sup> with the intensities corrected for Lorentz factor, polarization, air absorption, and absorption due to variation in the path length through the detector faceplate. Multi-scan absorption corrections were applied. The structures were solved by direct methods and refined on  $F^2$  by full matrix least squares using SHELXTL.<sup>S3</sup> All the non-hydrogen atoms were located from the Fourier maps, and were refined anisotropically. In the structural refinement of **3**, PART was used to refine disordered F atoms in  $\text{CF}_3\text{COO}^-$  anion. All H atoms were put in calculated positions using a riding model, and were refined isotropically, with the isotropic vibration parameters related to the non-H atom to which they are bonded. The crystallographic data for compounds **1-3** and **3-dimer·2DMF** are listed in Table 1, and selected bond lengths are given in Tables S1 and S2. CCDC 1415320–1415323 contain the supplementary crystallographic data for this paper. These data can be obtained free of charge from the Cambridge Crystallographic Data Centre via [www.ccdc.cam.ac.uk/data\\_request/cif](http://www.ccdc.cam.ac.uk/data_request/cif)

### The details of quantum chemical calculations

To simulate the fluorescence emissions of **1-3** in the condensed phase, we first performed quantum mechanics/molecular mechanics (QM/MM) geometry optimizations for an  $\text{anbdtiH/anbdtiH}_2^+$  molecule in a model cluster environment (including the central  $\text{anbdtiH/anbdtiH}_2^+$  molecule and its two nearest-neighbor  $\text{anbdtiH/anbdtiH}_2^+$  molecules as well as the nearby solvent molecules), in which the central  $\text{anbdtiH/anbdtiH}_2^+$  molecule is optimized at the first excited state ( $S_1$ ) using the time-dependent density functional theory (TDDFT) at CAM-B3LYP/6-31G(d,p) level and all the other atoms are frozen at the crystal structure and described by UFF force field. Then we performed the excited state calculation and the natural transition orbital (NTO) analysis for the whole cluster at the QM/MM optimized geometry. All

the calculations are performed by using Gaussian 09 program package.<sup>S4</sup>

**Table S1** Selected bond lengths (Å) for **1-3**

	<b>1</b>	<b>2</b>	<b>3</b>
N1-C15	1.317(6)	1.321(3)	1.336(3)
N2-C15	1.351(6)	1.346(3)	1.331(3)
N1-C17	1.394(6)	1.387(3)	1.389(2)
N2-C16	1.385(6)	1.380(3)	1.387(2)
O2-C31			1.247(3)
O1-C31			1.221(3)

**Table S2** Selected bond lengths (Å) for **3-dimer·2DMF**

C15-N1	1.321(5)	C1-C15	1.514(5)
C15-N2	1.363(5)	C1-C8A	1.624(5)
N1-C16	1.394(5)	N2-C17	1.385(5)

Symmetry code A:  $-x + 1, -y + 2, -z + 1$

**Table S3** Solid-state emission data of **1-3** at room temperature before and after grinding.

Compound	Before grinding	After grinding
<b>1</b>	488, 539, 603 nm	520 nm
<b>2</b>	453 nm	473 nm
<b>3</b>	533 nm	479, 505 nm

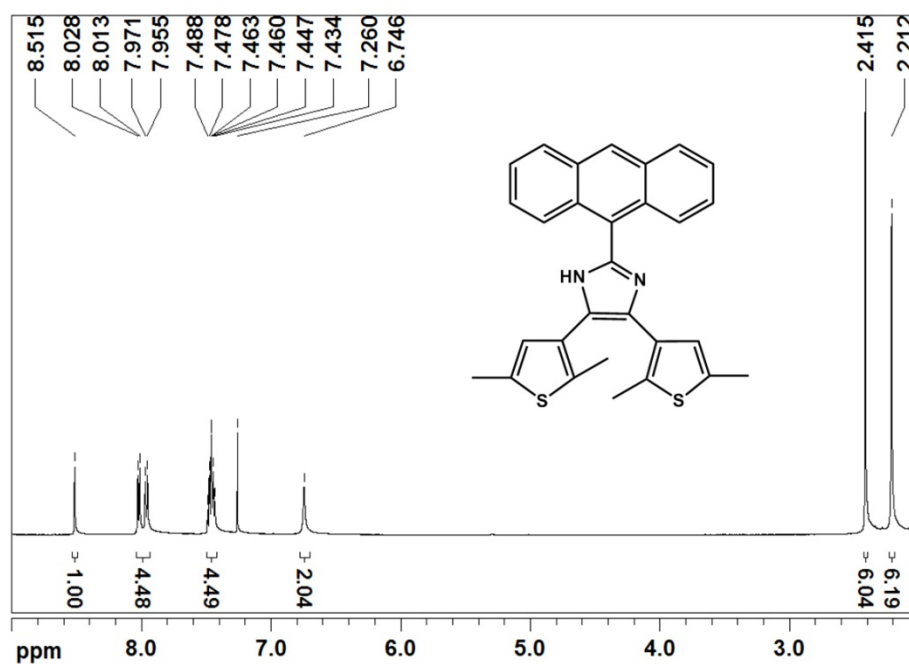


Fig. S1  $^1\text{H}$  NMR spectrum of anbdth (500 MHz,  $\text{CDCl}_3$ ).

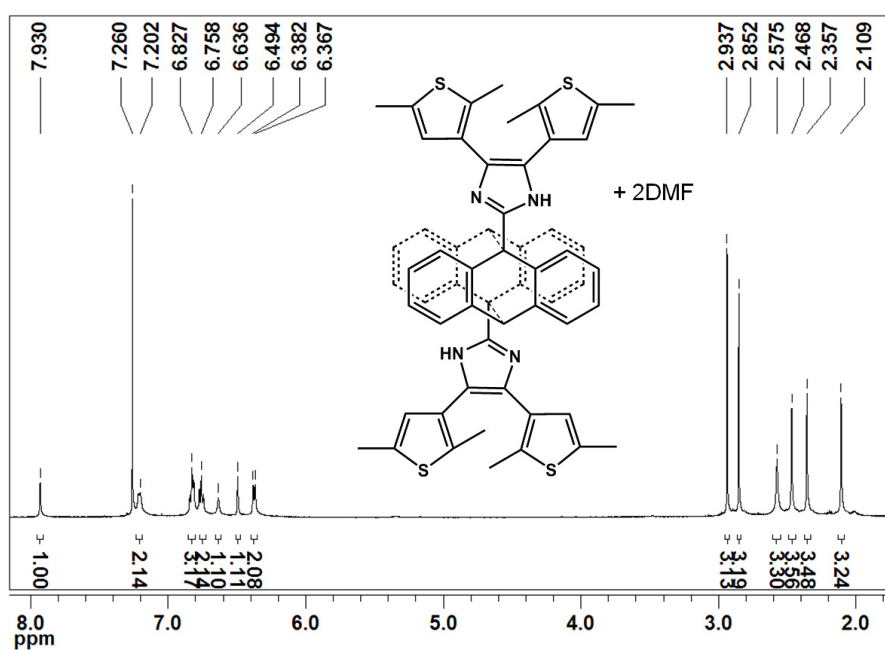
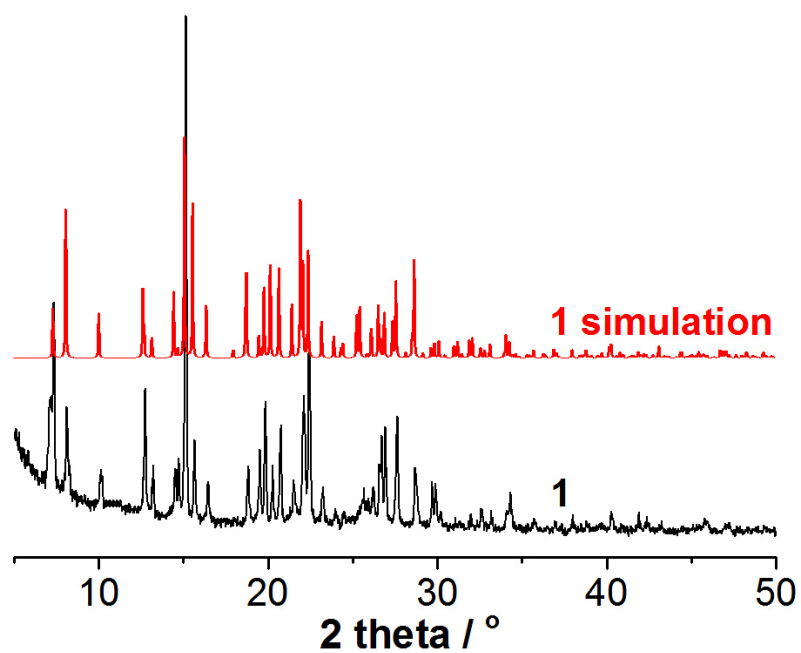
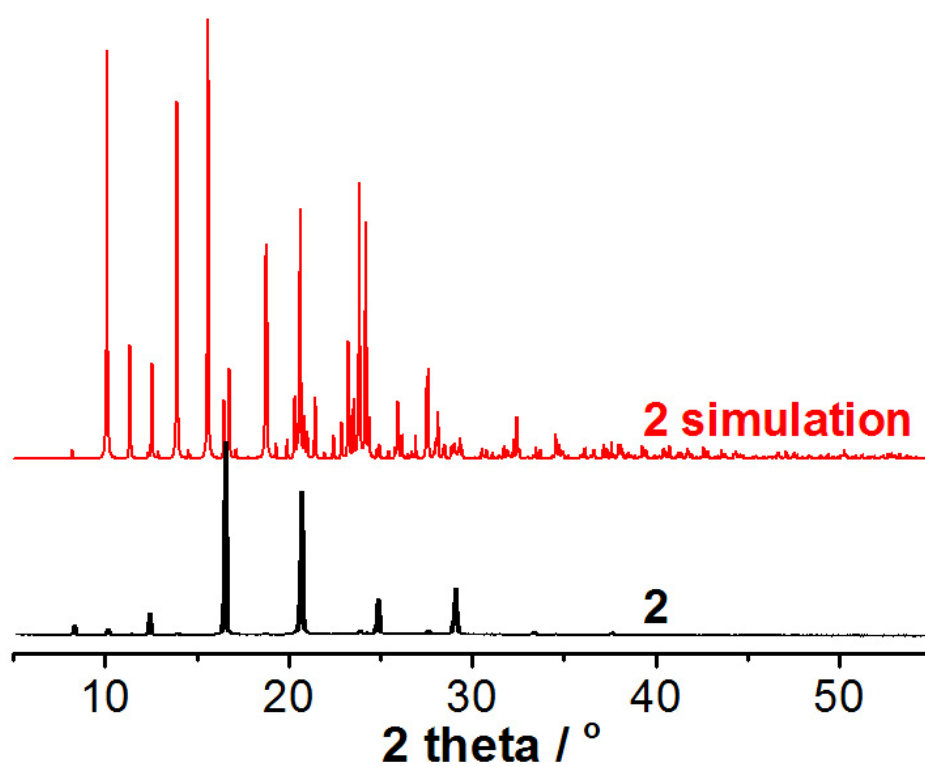


Fig. S2  $^1\text{H}$  NMR spectrum of 3-dimer-2DMF (500 MHz,  $\text{CDCl}_3$ ).



**Fig. S3** Experimental and simulated XRD patterns of 1.



**Fig. S4** Experimental and simulated XRD patterns of 2.

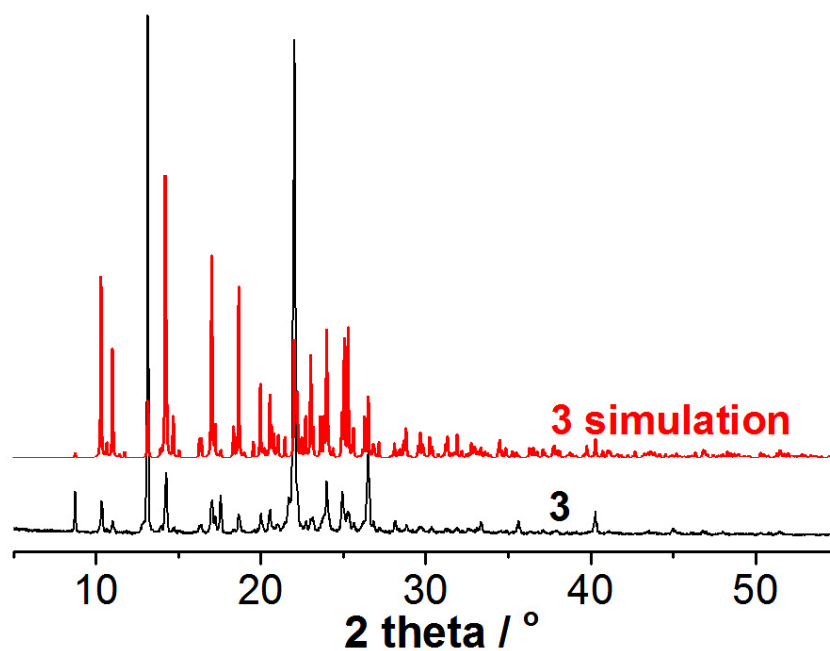


**Fig. S5** Experimental and simulated XRD patterns of **3**.

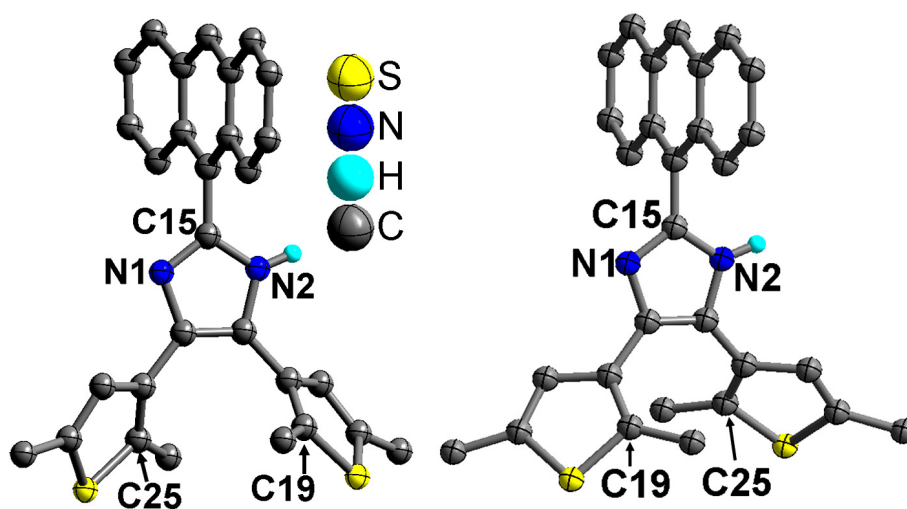


**Fig. S6** Structural units of **1** (left) and **2** (right). All H atoms attached to carbon atoms, and solvent molecules are omitted for clarity.



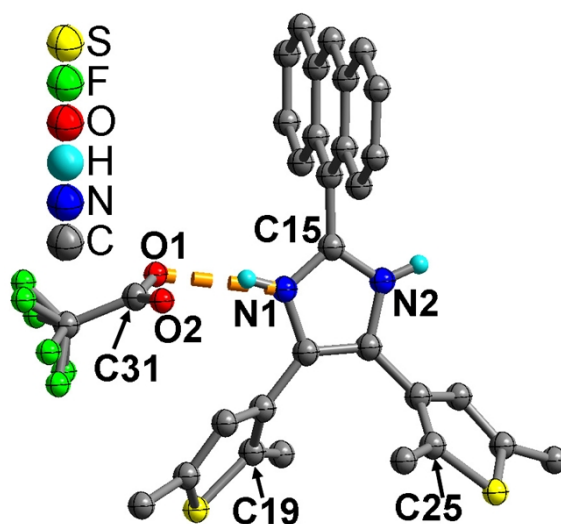


**Fig. S7** Structural unit of **3**. All H atoms attached to carbon atoms and lattice  $\text{CH}_3\text{OH}$  and  $\text{H}_2\text{O}$  molecules are omitted for clarity.

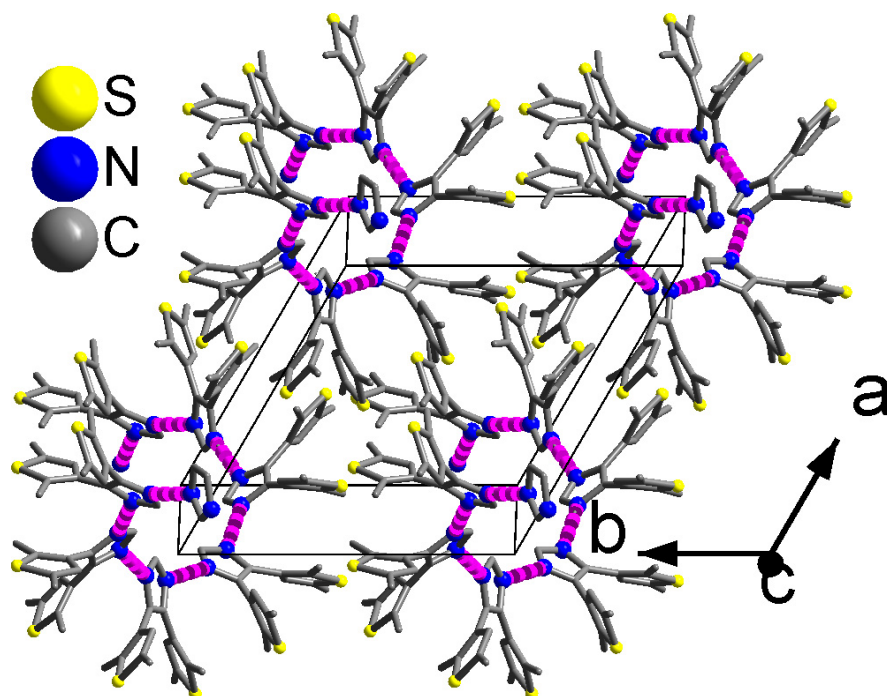


**Fig. S8** Packing structure of **1**. All anthracene groups and lattice  $\text{CH}_3\text{Cl}$  molecules are omitted for clarity.

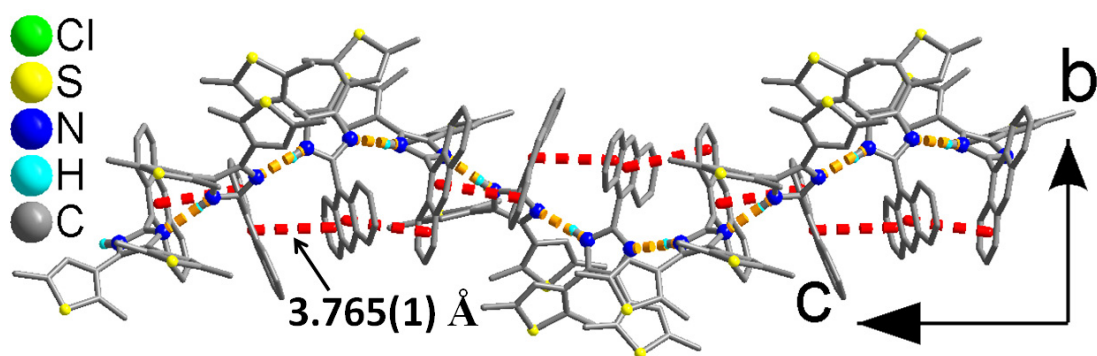


**Fig. S9** Supramolecular chain structure in **1** showing a centroid–centroid distance of 3.765(1) Å between two benzene rings from neighboring anthracene moieties.

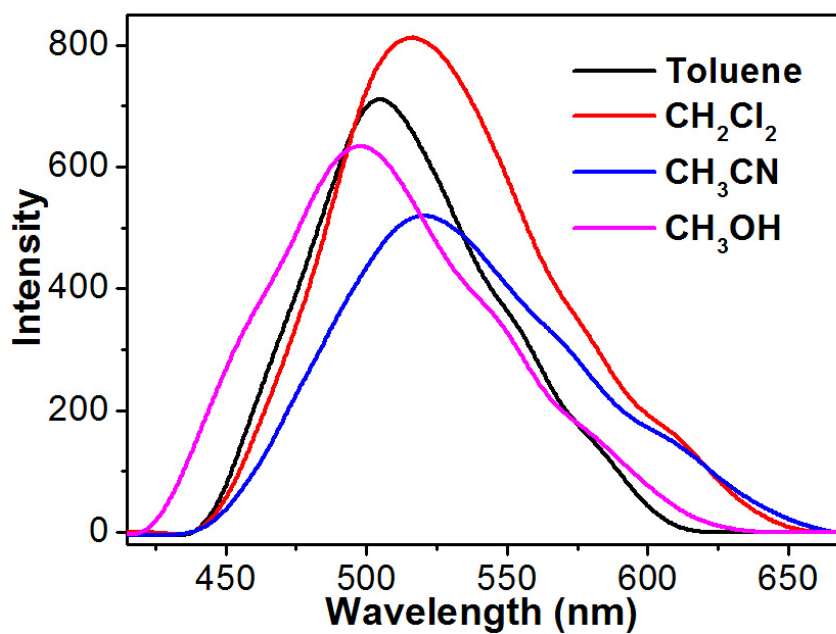


**Fig. S10** Luminescence spectra of anbdthH at room temperature in toluene, CH<sub>2</sub>Cl<sub>2</sub>, CH<sub>3</sub>CN and CH<sub>3</sub>OH ( $\lambda_{\text{ex}} = 380$  nm,  $c = 1 \times 10^{-4}$  M).

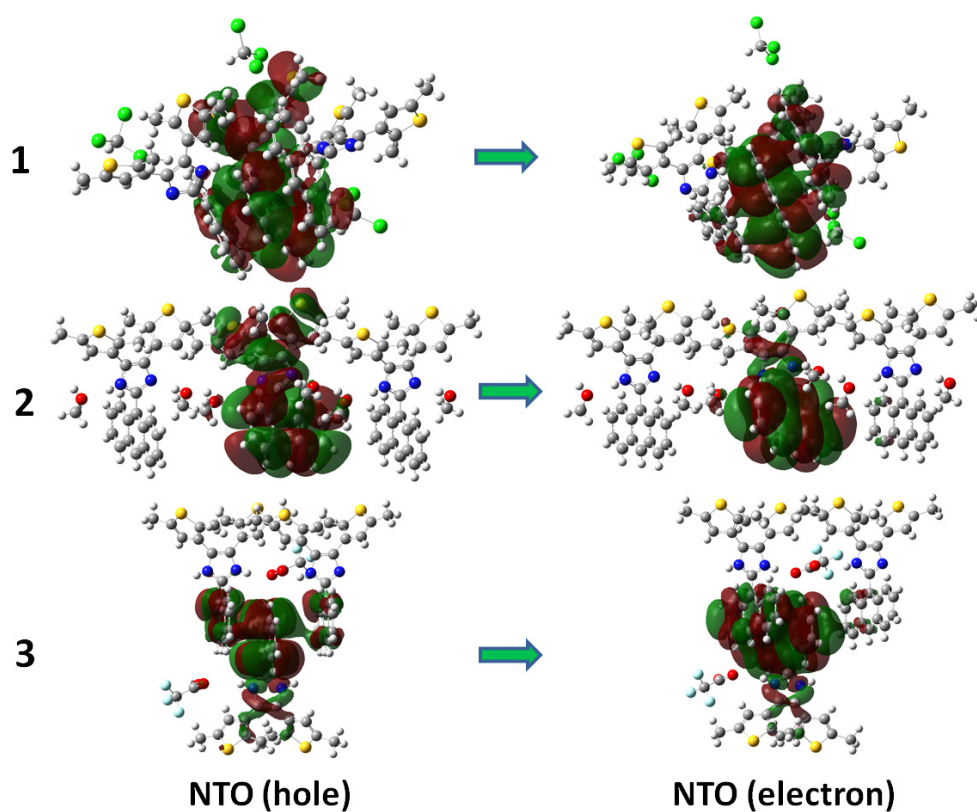


**Fig. S11** Natural transition orbitals (NTOs) for the first dipole-allowed excited state in model clusters of compounds **1-3** calculated at CAM-B3LYP/6-31G(d,p) level.

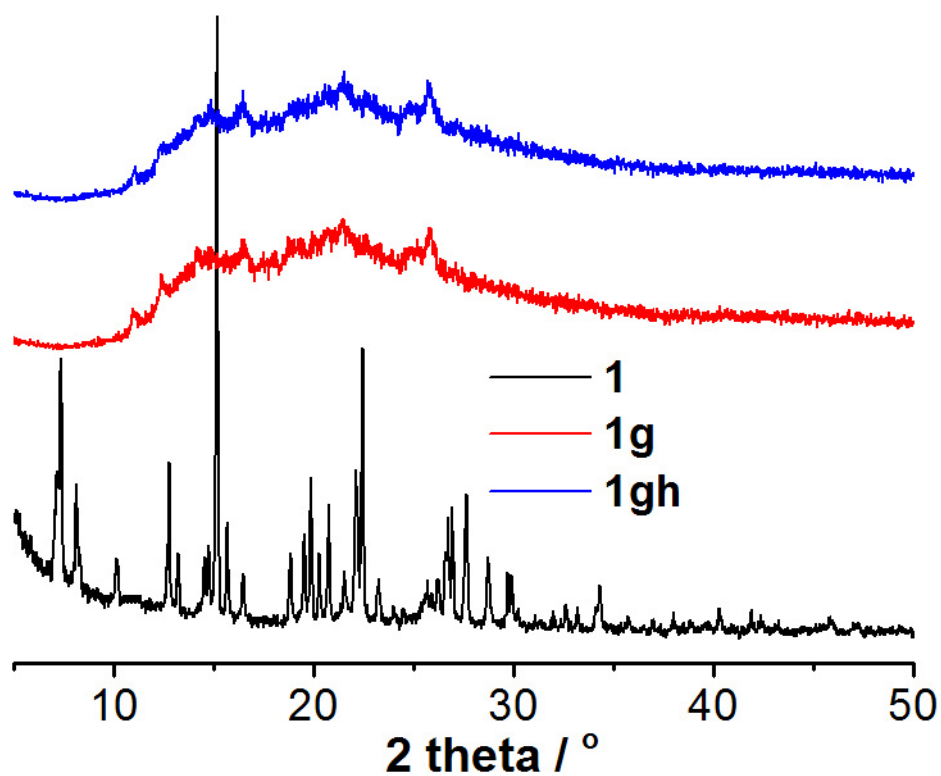


**Fig. S12** Experimental XRD patterns of **1**, **1g** and **1gh**.

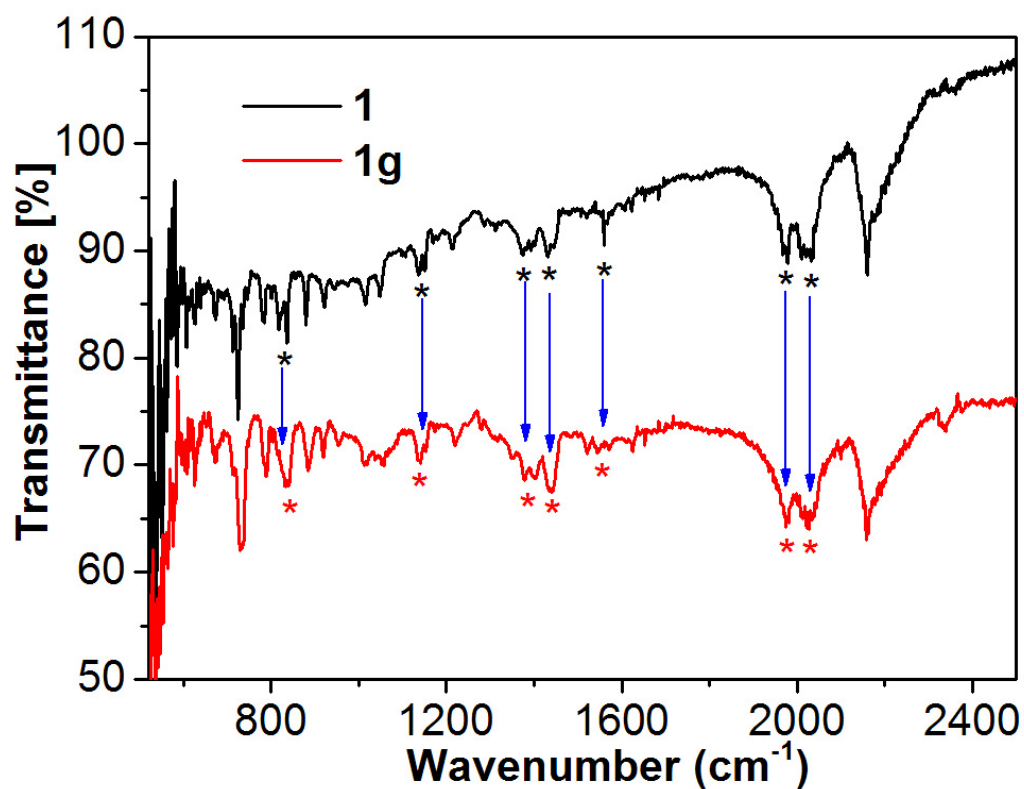


**Fig. S13** The ATR IR spectra of **1** and **1g**. \* = selected peaks indicating the differences between these compounds.

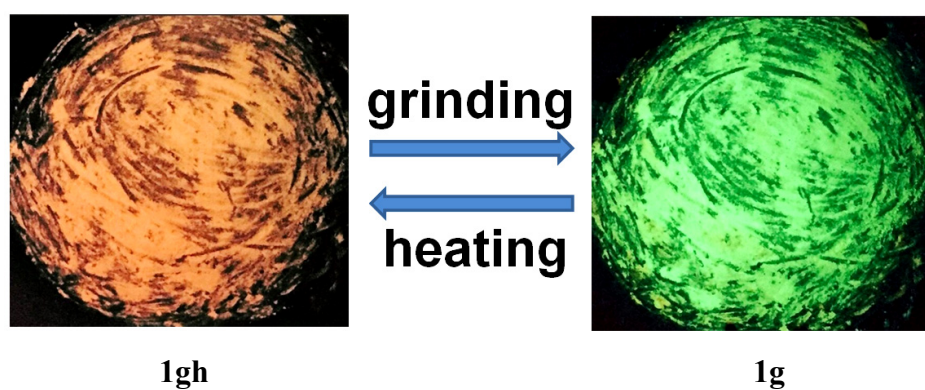


**Fig. S14** The emission colors of **1g** and **1gh** under the lamp with 365 nm wavelength.

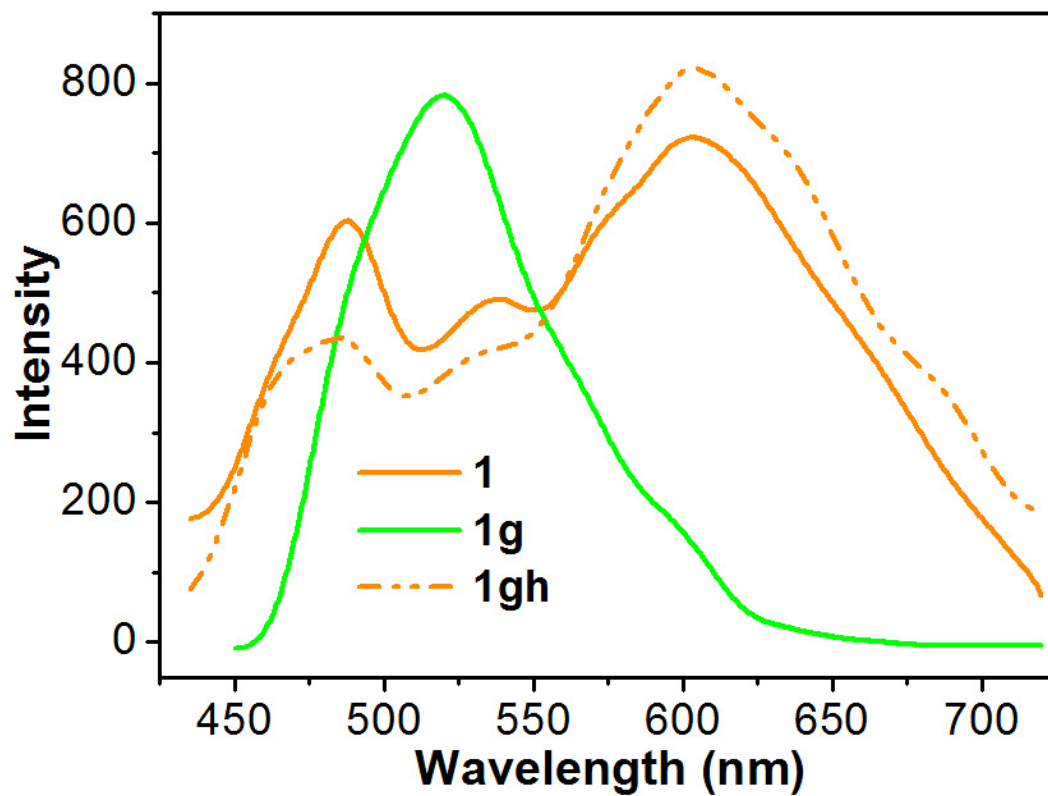


**Fig. S15** Solid-state luminescence spectra ( $\lambda = 380$  nm) of **1**, **1g** and **1gh** at room temperature.

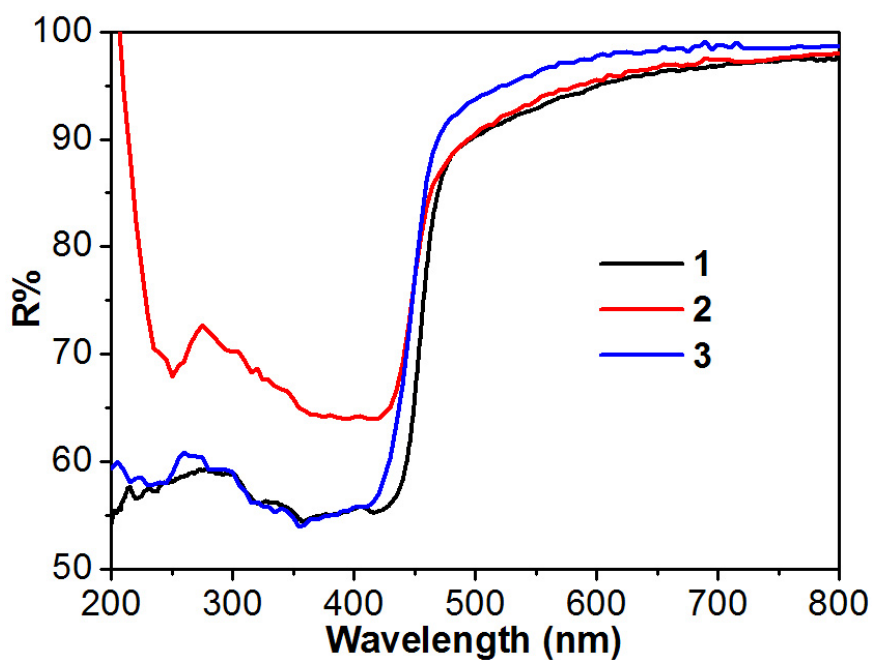


**Fig. S16** Diffuse reflectance spectra of **1-3** using barium sulfate as the reference.

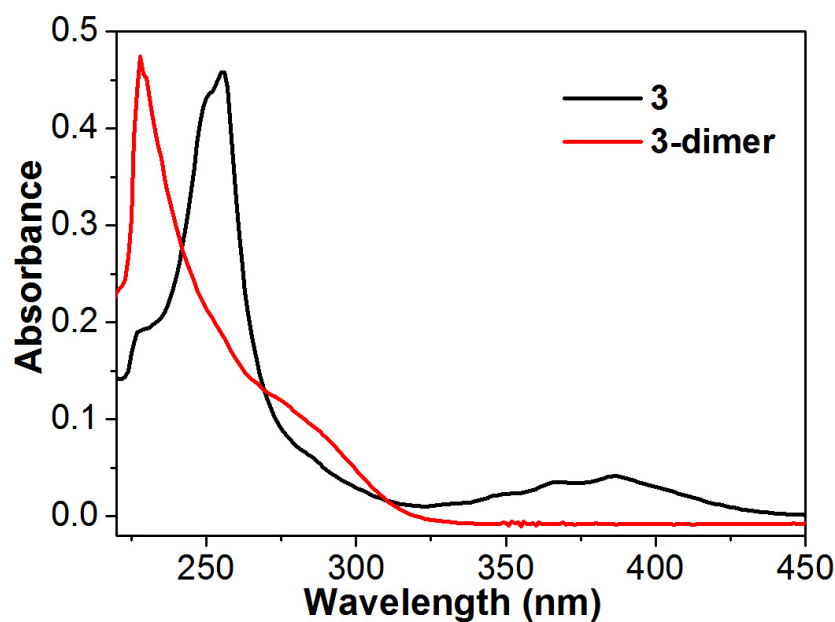


**Fig. S17** UV-vis spectra of **3** and **3-dimer** in CH<sub>2</sub>Cl<sub>2</sub> ( $c = 1.0 \times 10^{-5}$  M).

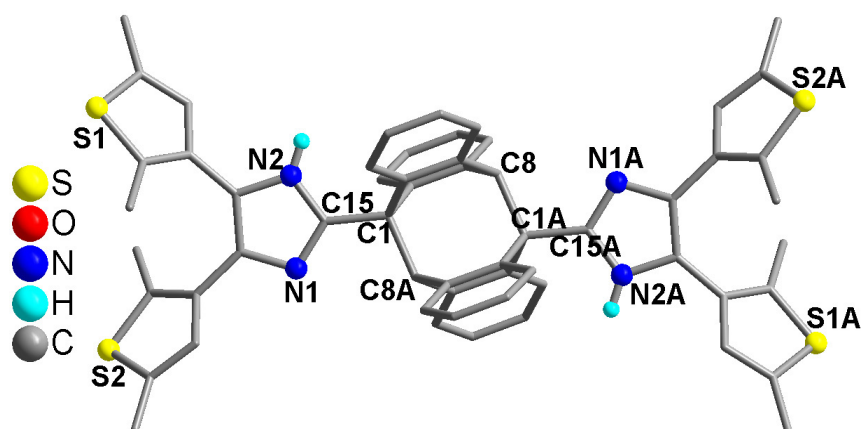


**Fig. S18** Molecular structure of **3-dimer·2DMF**. All H atoms attached to C atoms and two lattice DMF molecules are omitted for clarity.

## References

- S1 M. M. Krayushkin, S. N. Ivanov, A. Yu. Martynkin, B. V. Lichitsky, A. A. Dudinov, B. M. Uzhinov, *Russ. Chem. Bull., Int. Ed.*, 2001, **50**, 116.
- S2 *SAINT, Program for Data Extraction and Reduction*; Siemens Analytical X-ray Instruments: Madison, WI, 1994-1996.
- S3 (a) *SHELXTL, Reference Manual*, version 5.0; Siemens Industrial Automation, Analytical Instruments: Madison, WI, 1997. (b) G. M. Sheldrick, *Acta Crystallogr.*

*A*, 2008, **64**, 112.

S4 M. J. Frisch, G. W. Trucks, H. B. Schlegel, G. E. Scuseria, M. A. Robb, J. R. Cheeseman, G. Scalmani, V. Barone, B. Mennucci, G. A. Petersson, H. Nakatsuji, M. Caricato, X. Li, H. P. Hratchian, A. F. Izmaylov, J. Bloino, G. Zheng, J. L. Sonnenberg, M. Hada, M. Ehara, K. Toyota, R. Fukuda, J. Hasegawa, M. Ishida, T. Nakajima, Y. Honda, O. Kitao, H. Nakai, T. Vreven, J. A. Montgomery, Jr., J. E. Peralta, F. Ogliaro, M. Bearpark, J. J. Heyd, E. Brothers, K. N. Kudin, V. N. Staroverov, R. Kobayashi, J. Normand, K. Raghavachari, A. Rendell, J. C. Burant, S. S. Iyengar, J. Tomasi, M. Cossi, N. Rega, J. M. Millam, M. Klene, J. E. Knox, J. B. Cross, V. Bakken, C. Adamo, J. Jaramillo, R. Gomperts, R. E. Stratmann, O. Yazyev, A. J. Austin, R. Cammi, C. Pomelli, J. W. Ochterski, R. L. Martin, K. Morokuma, V. G. Zakrzewski, G. A. Voth, P. Salvador, J. J. Dannenberg, S. Dapprich, A. D. Daniels, Ö. Farkas, J. B. Foresman, J. V. Ortiz, J. Cioslowski, and D. J. Fox, Gaussian, Inc., Wallingford CT, 2009.